Neuropathology and Applied Neurobiology (2017), **43**, 358–365 doi: 10.1111/nan.12368

Scientific correspondence

Deregulated expression of *EZH2* in congenital brainstem disconnection

Congenital brainstem disconnection (CBSD) is an enigmatic embryo-fetal defect presenting as (sub)total absence of a segment between mesencephalon and lower brainstem. Rostro-caudal limits of the defect vary while the basal pons is always involved and the cerebellum is globally hypoplastic. A recent update and review [1] lists 14 cases, including three brain autopsy studies [1–3]. Necrosis and glial or inflammatory reactions were absent. Inferior olivary nuclei were small or absent, pontine nuclei depleted and the cerebellar dentate nuclei dysplastic. Supra-tentorial parts were normal in size, shape and microscopic structure. Frequent associated findings were vertebral segmentation defects (4/14) and hydronephrosis (3/14). No intra-familial recurrence or consanguinity was recorded.

We considered interference with the developing rhombencephalon by an epigenetic mechanism as possible cause of CBSD. We probed the role of PRC2 (Polycomb Repressive Complex 2), member of the polycomb group of chromatin modifying proteins (PcG) with a cell-fate conserving function in organ development [4–7]. PRC2 acts by promotor binding as well as by modification of histone H3 through its catalytic subunit EZH2 (Enhancer of Zeste2) that tri-methylates the free ending tail of H3 at lysine 27 to H3K27me3 (with H3K27me2 as intermediate step). H3K27me3 blocks transcription of developmental genes to consolidate the mature stage of cell lineage on completed development [7]. Advantageous use can be made of anti-H3K27me3 antibody staining of nuclear chromatin on routinely prepared autopsy tissue sections to study EZH2 activity, an application more commonly used in neoplastic studies [8], but not routinely applied in human malformations. The absence of immunoreactivity in a developmental setting is due to immaturity, as in embryonic stem cells, or to an abnormal persistence (or even reversal) to that state with loss of control over tissue-specific development. A large number of genes are known to undergo maturational silencing by histone modification. For example, EZH2 stabilizes the identity of individual vertebral body segments as well as brainstem development by silencing *HOX* genes [9,10]. Another role for EZH2, sustaining normal pontine neuron migration from the embryonic rhombic lip to the mature site of function has been identified by rhombomere-specific knockout of EZH2 in mouse embryos [11]. This finding prompted this study.

Antibody staining to H3K27me3 on routinely prepared autopsy material was applied in this study to probe a possible role for EZH2. *In situ* hybridization of *EZH2* mRNA was used to monitor *EZH2* transcription at sites of negative H3K27me3 staining. Antibody staining to histone H3K14ac, which is independent of EZH2 was used as tissue quality control for histone staining.

We studied a new patient (case 1) and a previously published patient with CBSD [1] (case 2 in this report) for local involvement of EZH2. We included brain material from the first reported autopsy of pontine tegmental cap dysplasia (PTCD) [12] (case 3) because characteristic aspects of brainstem morphology in PTCD are similar to CBSD [12,13]. Prominent features linking these three patients are summarized in Table 1.

Clinical and neuropathological findings of the three patients are as follows.

Patient 1 is the second male child of nonconsanguineous parents of European ancestry. Birth at 35 weeks was normal following an uncomplicated pregnancy. Birthweight was 2945 g, length 48.5 cm, head circumference 34 cm. Breathing was spontaneous. He had an absent gag reflex and hypertonia of jaw muscles. Radiographs showed multiple segmentation defects of the ribs and spinal column (Figure 1**D**). MRI of the brain on day 3 showed a defect separating the tegmentum from the ventral pons (Figure 1**A**,**B**) at the exit level of the trigeminal nerves. The cerebellum was normally shaped but hypoplastic (Figure 1**C**). He went home with tube feeding. At 8 months he was found dead at home by the parents. A coroner's autopsy was performed.

The copyright line for this article was changed on 23 August 2017 after original online publication

Table 1. Comparison of cerebral pathology of cases 1, 2 and 3

	Case 1 (patient 1)	*Case 2 (patient 2)*	*Case 3 (patient 3)*
Previously published data	None	Clinics and neuropathology: ref. [1]	Clinics and neuropathology: ref. [12]
Diagnosis	Congenital brainstem disconnection	Congenital brainstem disconnection	Pontine tegmental cap dysplasia
Gender	Male	Male	Male
Age at death	8 months	8 months	32 months
Undersized ventral pons	Yes	Yes	Yes
Ectopia of transverse pontine fibres	To anterior medullary velum of the cerebellum	No	To pontine tegmentum
Cerebellar hypoplasia	Yes	Yes	Yes
Absence of inferior olivary nuclei	Yes	Yes	Near absence
Dysplasia of the cerebellar dentate nuclei	Yes	Yes	Yes
Rim around lower brainstem devoid of neural tissue	Yes	Yes	No
Extracerebral organ involvement	Malformation of thoracic vertebral column and ribs Hydronephrosis	Left-sided ureteral reflux	Tetralogy of Fallot Bilateral clubfoot

With legal and parental consent formalin-fixed specimens of the brain were made available for this study.

General autopsy revealed bilateral hydronephrosis. The fresh brain weight was 745 g. The midbrain was present but the pons was only 1.5 cm in diameter with a nodular shape. The junction between pons and medulla was just 0.5 cm in diameter. Histopathological examination after routine staining demonstrated no abnormalities in any supra-tentorial structures.

Immunohistochemistry was performed, as described [14]. The following antibodies were used in the routine immunohistochemical analysis of case 1: glial fibrillary acidic protein (GFAP; polyclonal rabbit, DAKO, Glostrup, Denmark; 1:4000; monoclonal mouse, 1:50; DAKO), Synaptophysin (mouse clone SY38, 1:200; DAKO); microtubule- associated protein (MAP2; mouse clone HM2, 1:100; Sigma, St. Louis, Mo, USA), SMI 311: monoclonal mouse (Sternberger monoclonals) 1:000, MBP (myelin binding protein) 1:400, DAKO.

Brainstem sections stained with antibodies to MBP and SMI 311 revealed an abnormal course of the cortico-ponto-cerebellar tracts: instead of joining the ventral pons each of these followed a circular route at the surface of the lower mesencephalon to end up in the anterior medullary velum of the cerebellum (Figure 1**E**–**H**). The cerebral peduncles were normally myelinated but too small. The decussation of the superior cerebellar peduncles was indistinct. The pontine tegmentum bordering the fourth ventricle lacked a midline depression separating left and right halves. A large smooth edged defect separated the pontine tegmentum from the ventral pons. The middle cerebellar peduncles were absent and the trigeminal roots could be identified at the upper margin of the defect. At the same transverse level, a disc with a smooth margin and diameter of 8 mm represented the ventral pons (Figure 1**I**) in which the pyramidal tracts could be identified. The structure dorsal to the pyramidal tracts contained sparse transverse fibres, few neurons and lacked a midline raphe. The medulla oblongata appeared more normal. The inferior cerebellar peduncles were diminished in size. The medial lemnisci were indistinct. The pyramids were present. The sites of the inferior olivary nuclei were empty (Figure 1**J**). An abnormal rim was seen surrounding the lower brainstem, immunonegative for axons (SMI311) (Figure 1**I**, **J**), but immunopositive for glial staining (GFAP, not shown). The cerebellar cortex was normal on routine staining, but the cerebellar dentate nucleus lacked its continuous undulated structure, instead appearing as collections or aggregates of neurons resembling islands (Figure 1**K**).

The spinal cord was not available for study. The routine neuropathological results are summarized in Table 1 together with those from patients 2 and 3.

Patient 2: The clinical and cerebral post-mortem findings were extensively reported [1] and are summarized here. He was clinically diagnosed as having CBSD by

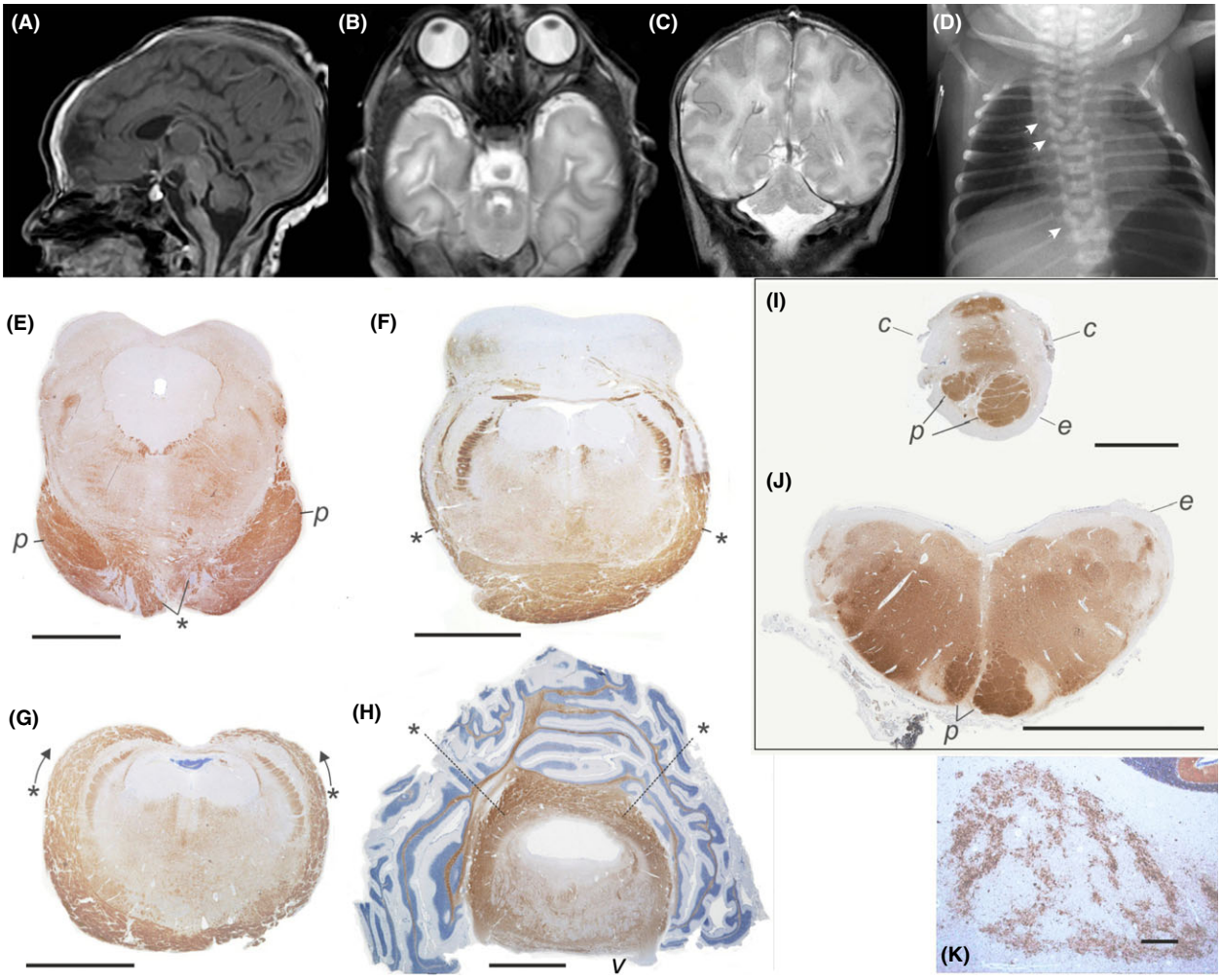

Figure 1. Neuro-imaging and routine neuropathology (case 1). (**A**–**C**) Neonatal MRI of the brain. (**A**) Midsagittal section showing partial brainstem disconnection at pontine level. (**B**) Coronal section showing separation of diminutive ventral pons and pontine tegmentum at exit level of trigeminal nerve. (**C**) Coronal section showing a normally proportioned, hypoplastic cerebellum. (**D**) Neonatal thoracic X-ray showing segmentation anomalies indicated by arrows. (**E**–**H**) Consecutive transverse histological sections from inferior colliculi to pontine tegmentum showing deviant course of cortico-pontine precerebellar fibres on both sides indicated by asterisk (*): superficial to the lower mesencephalon, with upward and posteriorly directed course (**E**–**G**), ending in the anterior medullary velum of the cerebellum (**H**). Near absence of transverse pontine fibres and middle cerebellar peduncles (**H**). *p*, pyramidal tracts; *V*, trigeminal nerve root. Notice the absence of the median depression at the ventricular face of the pontine tegementum (**H**). MBP (myelin basic protein) antibody staining. (**I**) Pontine remnant, at autopsy ventral to section **H**. Approximate location visible on MRI section **B**. Paucity of transverse fibres. Median raphe absent in upper part, but present between asymmetric pyramidal tracts marked *p*. Choroid plexus marked *c*. SMI 311 axon staining. (**J**) Medulla oblongata with median raphe, pyramids, inferior cerebellar peduncles present and beds of inferior olivary nuclei depleted of neurons. SMI 311 axon staining. (**I**,**J**) Pontine remnant and medulla oblongata with superficial band marked *e* devoid of neural tissue. (**K**) Dysplastic cerebellar dentate nucleus with neurons grouped in masses, and absence of normal garland structure. Note 1: minor right-sided artificial damage to tissue in **F** graphically corrected. Note 2: superficial band surrounding pontine remnant and medulla oblongata positive for GFAP (not shown).

typical MRI findings and died at 8 months. Autopsy showed an abnormally small pons on cross section, mostly made up of tegmentum with a thin rim of ventral pons, which contained only sparse neurons. Nuclei of cranial nerves VI and VII were indistinct. Abnormal neuroglial tissue was present around the lower medulla.

Patient 3: This is the first patient diagnosed with PTCD whose brain pathology was reported in detail [12,13]. The case is included in this series because

brainstem morphologies of PTCD and CBSD share important features (Table 1).

Histone immunostaining and in situ hybridization was similarly performed in all three cases and controls: We used anti-Histone H3 (dimethyl K27; H3K27me2) antibody (ab24684; rabbit polyclonal, 1:500; Abcam, Cambridge, MA, USA), anti-trimethyl Histone H3 (Lys27; H3K27me3) antibody (rabbit polyclonal, 1:100; Millipore Billerica, MA, USA) and anti-Histone H3 (acetyl K14; H3K14ac) antibody (ab52946; rabbit monoclonal, 1:100; Abcam). *In situ hybridization* (ish) for *EZH2* was performed using – 5′ fluorescein labelled 19-mer antisense oligonucleotides containing Locked Nucleic Acid and 2′OME RNA moieties (*EZH2*: FAM-AguTucAucTucCacCauA); The oligonucleotides were synthesized by Ribotask ApS, Odense, Denmark. The hybridizations were done at 59°C on 6 μM sections of paraffin embedded tissue described previously [15]. The hybridization signal was detected using anti-fluorescein AP-labelled FAB fragments (11 426 338 910, Roche Diagnostics, Almere, the Netherlands). Signal was detected with Vector Alkaline Phosphatase Substrate kit III (Vector laboratories Inc. CA 94010 USA SK-5300). Nuclear counterstaining was done using nuclear fast red solution (N3020; Sigma).

We obtained the following results for specific histone staining and *EZH2 in situ* hybridization (Figure 2). In controls, H3K27me3 immunoreactivity was strong in nuclei of cerebellar cortex (all layers), cerebellar dentate nucleus (not shown) and temporal cerebral cortex (Figure 2**A**–**D**). In *case 1*, H3K27me3 immunoreactivity was undetectable in the cerebellar cortex and dentate nucleus (Figure 2**E**,**F**); expression was reduced in both internal and external granular cell layer and Purkinje cells; H3K27me3 signal was observed in other brain areas including temporal cortex (Figure 2**G**). Areas rostral and caudal to the affected brainstem segment showed H3K27me3 immunopositivity in cellular nuclei and immunonegativity in the sparse remaining neurons of the pons (not shown). The nuclear pattern of H3K14ac immunoreactivity was preserved in cerebellum confirming tissue quality for general histone staining (Figure 2**H**). Results for H3K27me2 were identical to those for H3K27me3 and therefore not shown. *In case 2* H3K27me3 immunoreactivity was reduced in cerebellar cortex (Figure 2**I**,**J**) with nuclear staining in a small quantity of internal granule cells and molecular layer cells, while it was well presented in temporal cerebral cortex (Figure 1**K**). H3K14ac staining was preserved in case 2 (Figure 2**L**). H3K27me3 immunopositivity was also found in mesencephalon and medulla oblongata in areas flanking the affected pontine region. Not enough ventral pontine neurons were available for reliable histone mapping. *In case 3*, nuclear H3K27me3 was observed in brain in all areas including the cerebellum, in contrast to the CBSD cases. (PTCD; Figure S1**A**–**C**). In all three cases paired results using two different batches of anti H3K27me3 antibody were similar. Results for H3K27me2 were identical to those for H3K27me3 in all three cases, and therefore not shown. *In situ hybridization of EZH2* in control cerebellum showed strong uniform expression in Purkinje cells (Figure 2**M**); neuronal *EZH2* expression was also detected in temporal cortex (not shown). *In case 1*, *EZH2* expression was absent in Purkinje cells (Figure 2**N**); however, normal *EZH2* expression was observed in other brain areas (not shown, but similar to case 2). *EZH2* expression was also reduced in the cerebellum from *case 2* (Figure 2**O**); marginally positive expression was found in a few samples, but less than temporal cortex (Figure 2**P**) or control cerebellum (Figure 2**M**).

Studies on DNA obtained from blood samples in the two patients with brainstem disconnection and their parents excluded a mutation in the *EZH2* gene except for

Figure 2. H3K27me3, H3K14ac immunoreactivity and *in situ* hybridization of EZH2 mRNA in control and congenital brainstem disconnection (CBSD) cases 1, 2. (**A**–**D**) Control, age 9 months. (**A**,**B**) (cerebellum): H3K27me3 immunopositive in external and internal granule cell layers and Purkinje cell nuclei (arrows in **B**). (**C**) Temporal cortex: H3K27me3 immunopositive in layer II–III nuclei. (**D**) H3K14ac immunopositive in external and internal granule cell layers and Purkinje cell nuclei (arrows). (**E**–**H**) Case 1 CBSD case. (**E**,**F**) Cerebellum: H3K27me3 undetectable in external and internal granule cell layers and Purkinje cells (arrows and insert in **F**). (**G**) Temporal cortex: layer II–III, immunopositive nuclei. (**H**) H3K14ac immunopositive in internal granule cell layer and Purkinje cells (arrows). (**I**–**L**) Case 2 CBSD case. (**I**,**J**) Cerebellum: H3K27me3 nearly absent in external and external granule cell layers and Purkinje cells (arrow and insert in **J**) with sparse immunopositive nuclei in molecular layer. (**K**) Temporal cortex: layer II–III, immunopositive nuclei. (**L**) Cerebellum: H3K14ac present in external and internal granule cell layers. The sections were counterstained with haematoxylin. (**M**–**O**) *In situ* hybridization of EZH2 in control cerebellum (**M**) and cases 1 and 2 (**N**,**O**). The sections were counterstained with fast red. (**M**) (control): positive expression in Purkinje cells (arrows and insert). (**N**) Case 1: no expression in Purkinje cells (arrows and insert). (**O**) Case 2: markedly diminished expression (insert shows a negative Purkinje cell). (**P**) Case 2: positive expression in temporal cortex. Scale bar in **P**: **A**: 160 μm; **E**, **I**, **H**, **L**: 320 μm; **B**–**D**,**F**,**G**,**J**,**K**,**M**–**O**: 80 μm; **P**: 60 μm.

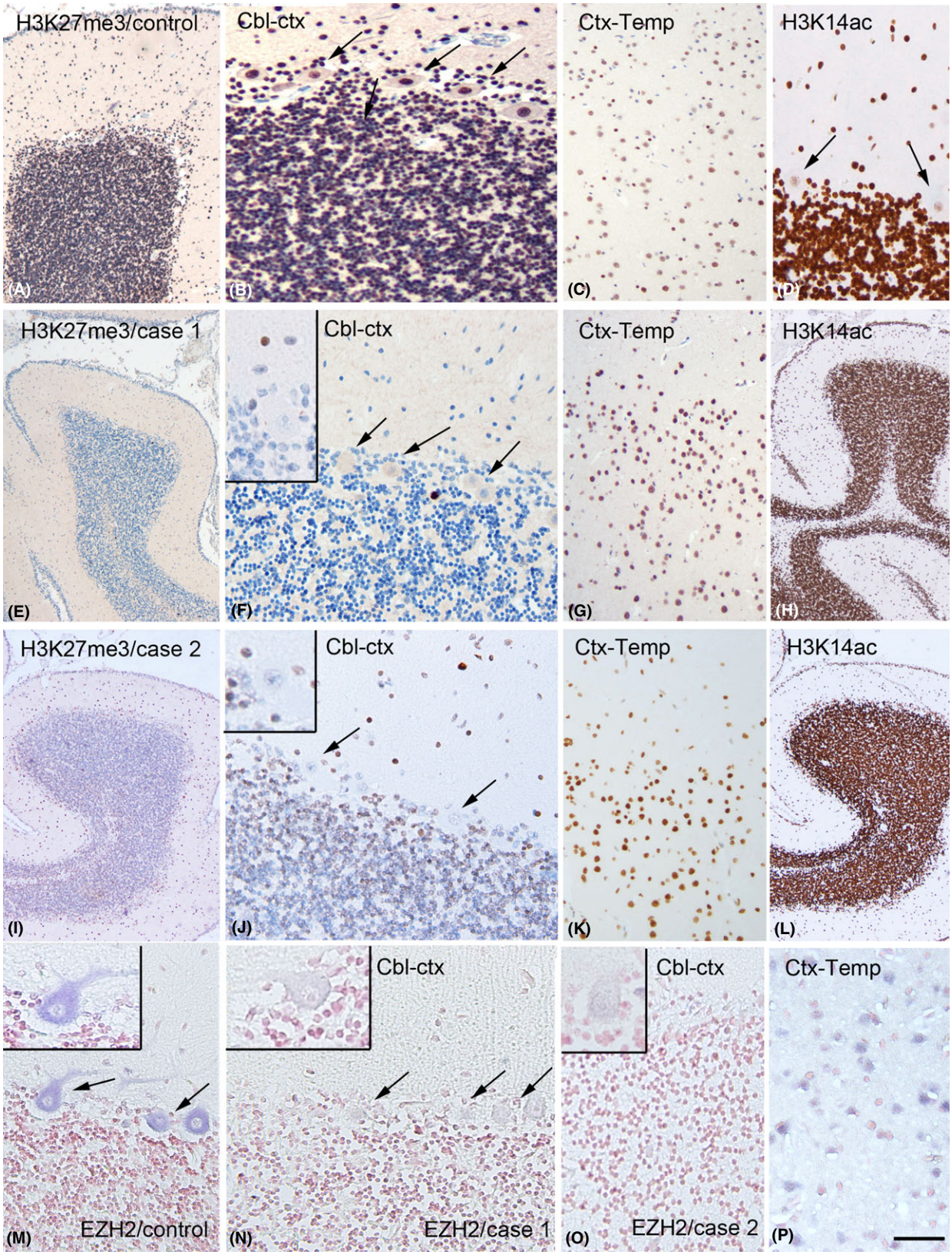

known reported polymorphisms. For case 1, whole genome analysis of DNA isolated from fibroblasts of the patient was performed. We evaluated all introns and noncoding parts as well as the surrounding 530 kb region of the *EZH2* gene. No obvious pathogenic mutations or partial deletions were detected.

Experimental knockout of the Ezh2 gene from rhombomeric regions in embryonic mice [11] impedes the migration of pontine precerebellar neurons causing heterotopia. The stalled migration is not intrinsic, that is, not due to changed properties of the migrating neurons, but due to loss of migratory guidance in which Ezh2 has an 'orchestrating' role [11]. This takes effect in two ways: (i) by limiting the Sonic hedgehog pathway, which controls the distribution of the chemo-attractant and guidance factor Netrin-1, to the floor plate region. (ii) By restricting the migrating neurons to different HOX (that is, homeobox related) regions. Rescue innervation of the ectopic neurons through their proper afferents (from the cerebral cortex), a precondition for their survival, was also demonstrated in the murine knockout [11]. In CBSD, no collections of ectopic pontine neurons were found. Instead ventral pontine nuclei were almost absent in the present as well as in previously reported CBSD cases. The most likely explanation holds that in CBSD, inappropriate guidance of migrating pontine neurons is compounded by failed rescue innervation, resulting in cell death by apoptosis. This explanation is strengthened by a detail in case 1, not previously encountered in CBSD: the ectopic cortico-pontine fibre tracts, misdirected to the anterior medullary velum (Figure 1**H**). No collection of ectopic neurons was found there. The heterotopic cortico-pontine tracts signify that pontine nuclei were not normally innervated by afferents from the cerebral cortex at *any* time from the moment of their origin. Incidentally, the abnormal tracts signify axon misrouting, a process which partly relies on a gradient of the chemo-attractant Netrin-1 for the directed outgrowth of neurites, which is similar to the process by which migrating young neurons are guided at an earlier stage [16]. No experimental data exist on the impact of the loss of EZH2 on the migration of future inferior olivary neurons. These neurons also originate in the rhombic lip, and are similarly guided by the presence of Netrin-1 [17] in the floor plate; therefore, likely to be affected by loss of migratory control in the case of lost EZH2 function. The loss of pontine and inferior olivary neurons precluded their use to test the presence of H3K27me3. Reliable histone typing in brainstem nuclei was impeded by altered anatomy. By good fortune, the cerebellum, which belongs to the embryonic rhombencephalon [18] was sufficiently preserved, presenting a homogenous cell-rich structure that could be used for histone testing with consistent results. In a recent study in embryonic mice, targeted knockout of EZH2 from the future cerebellar region [19] resulted in global hypoplasia. The loss of EZH2 affected cerebellar precursor cells from both the rhombic lip and the

Table 2. EZH2: multiple roles in development of the nervous system and vertebral column

Embryonic brain	*Functions of EZH2 in brain development*	*Loss of EZH2 in experiments*	*References*
All parts	Reversible blockage of transcription of selected genes in embryonic stem cells, neural stem cells and neurons allowing sequential order in development of neural cell lineages (neurons, astrocytes, oligodendroglia)	Altered ratios of neurons and astroglia	[6,7,20]
Rhombencephalon	Directing pontine neuron migration from rhombic lip to pontine nuclei: 1. By indirect action on Netrin-1 distribution through Sonic hedgehog, causing ventral migration route 2. Through action on HOX proteins, limiting rostro-caudal distribution	Failure of Netrin-1-guided neuron migration causes heterotopia of pontine precerebellar neurons with rescue of cortico-pontine innervation. Possible similar effect on olivary nuclei	[11]
	Ventricular zone: Diversity of GABAergic neurons Rhombic lip: Proliferation granule cell precursors	Cerebellar hypoplasia	[19]
Somites	HOX genes silencing on completed differentiation, establishing vertebral identity	Vertebral segmentation defects	[9,10]

ventricular zone, respectively, resulting in loss of internal granule cells, an altered ratio between GABAergic neurons and loss of Purkinje cells. Histone staining results of the cerebellum for H3K27me3 were remarkably similar to the present cases of CBSD. Experimental loss of EZH2 also results in delayed HOX gene silencing, causing rhombomeric and vertebral segmentation defects [9,10]. The latter effect bears morphological similarity to vertebral segmentation defects as observed in patient 1 as well as a significant portion of published CBSD cases [1]. Table 2 summarizes the multiple roles for EZH2 in the development of the nervous system and vertebral column as presently known.

In conclusion, this study of two cases of CBSD shows the involvement of EZH2 by the diminished presence of its enzyme product histone H3K27me3, throughout the cerebellum, as well as by the absence of EZH2 transcription in the same regions. Comparison to the results of experimental knockout of EZH2 by selective targeting of rhombomeres [11] well explains part of its unusual neuropathology, for example, the vanished pontine and inferior olivary nuclei. Also, cerebellar hypoplasia in CBSD compares well with experimental knockout of EZH2 from the future cerebellar region [19]. The mechanism by which this local gene dysregulation in early human embryogenesis is initiated in the apparent absence of systemic genomic mutations remains to be addressed. A case of PTCD, studied because of important morphologic similarities to CBSD was unaffected by histone changes.

Acknowledgements

The authors thank Dr Steffen Albrecht, Department of Pathology, Montreal Neurological Institute and the Montreal Children's Hospital, Montreal, Canada for providing the material for study of case 1. We acknowledge Prof. Evelyne Bloch-Gallego, Institut Cochin, Inserm, Paris, France, for helpful theoretical discussion.

Author contributions

P. G. Barth: neuropathology, basic literature search, concept of present study. E. Aronica: neuropathology, immune-typing and *in situ* hybridization. S. Fox: clinical genetics and clinical data case 1. K. Fluiter: *in situ* hybridization. M. A. J. Weterman: Sanger sequencing, whole genome sequencing. A. Poretti: neuroradiology, patient data case 2. D. C. Miller: neuropathology case 2. E. Boltshauser: paediatric neurology, expertise cerebellar disorders, general discussion. B. Harding: neuropathology PTCD case 3. M. Santi: neuropathology PTCD case 3. F. Baas: supervision of the project.

P. G. Barth*,†[1]
E. Aronica†[1]
S. Fox‡
K. Fluiter§
M. A. J. Weterman§
A. Poretti¶
D. C. Miller**
E. Boltshauser††
B. Harding‡‡
M. Santi‡‡
F. Baas§

**Department of Pediatric Neurology, Emma Children's Hospital/Academic Medical Centre, †Department of (Neuro) Pathology, Academic Medical Centre, University of Amsterdam, Amsterdam, The Netherlands, ‡Department of Medical Genetics, McGill University Health Centre, Montreal, QC, Canada, §Department of Genome Analysis Clinical Genetics, Academic Medical Centre, University of Amsterdam, Amsterdam, The Netherlands, ¶Section of Pediatric Neuroradiology, Division of Pediatric Radiology, Russell H. Morgan Department of Radiology and Radiological Science, The Johns Hopkins University School of Medicine, Baltimore, MD, **Department of Pathology and Anatomical Sciences, University of Missouri School of Medicine, Columbia, MO, USA, ††Department of Pediatric Neurology, University Children's Hospital, Zurich, Switzerland and ‡‡Departments of Pathology and Lab Medicine (Neuropathology), Children's Hospital of Philadelphia and the Perelman School of Medicine, University of Pennsylvania, Philadelphia, PA, USA*

[1]These authors have made equal contributions to the work.

References

1 Poretti A, Denecke J, Miller DC, Schiffmann H, Buhk JH, Grange DK, Doherty D, Boltshauser E. Brainstem disconnection: two additional patients and expansion of the phenotype. *Neuropediatrics* 2015; **46**: 139–44
2 Sarnat HB, Benjamin DR, Siebert JR, Kletter GB, Cheyette SR. Agenesis of the mesencephalon and metencephalon with cerebellar hypoplasia: putative mutation in the EN2 gene – report of 2 cases in early infancy. *Pediatr Dev Pathol* 2002; **5**: 54–68
3 Barth PG, de Vries LS, Nikkels PG, Troost D. Congenital brainstem disconnection associated with a syrinx of the brainstem. *Neuropediatrics* 2008; **39**: 1–7

4 Margueron R, Reinberg D. The Polycomb complex PRC2 and its mark in life. *Nature* 2011; **469**: 343–9
5 Prezioso C, Orlando V. Polycomb proteins in mammalian cell differentiation and plasticity. *FEBS Lett* 2011; **585**: 2067–77
6 Aloia L, Di Stefano B, Di Croce L. Polycomb complexes in stem cells and embryonic development. *Development* 2013; **140**: 2525–34
7 Chou RH, Yu YL, Hung MC. The roles of EZH2 in cell lineage commitment. *Am J Transl Res* 2011; **3**: 243–50
8 Bechet D, Gielen GG, Korshunov A, Pfister SM, Rousso C, Faury D, Fiset PO, Benlimane N, Lewis PW, Lu C, David Allis C, Kieran MW, Ligon KL, Pietsch T, Ellezam B, Albrecht S, Jabado N. Specific detection of methionine 27 mutation in histone 3 variants (H3K27M) in fixed tissue from high-grade astrocytomas. *Acta Neuropathol*. 2014; **128**: 733–41.
9 Kim SY, Paylor SW, Magnuson T, Schumacher A. Juxtaposed Polycomb complexes co-regulate vertebral identity. *Development* 2006; **133**: 4957–68
10 Alexander T, Nolte C, Krumlauf R. Hox genes and segmentation of the hindbrain and axial skeleton. *Annu Rev Cell Dev Biol* 2009; **25**: 431–56
11 DiMeglio T, Kratochwil CF, Vilain N, Loche A, Vitobello A, Yonehara K, Hrycaj SM, Roska B, Peters AH, Eichmann A, Wellik D, Ducret S, Rijli FM. EZH2 orchestrates topographic migration and connectivity of mouse precerebellar neurons. *Science* 2013; **339**: 204–7
12 Harding B, Vossough A, Goldberg E, Santi M. Pontine tegmental cap dysplasia: neuropathologic confirmation of a rare clinical/radiologic syndrome. *Neuropathol Appl Neurobiol* 2016; **42**: 301–6
13 Barth PG, Majoie CB, Caan MW, Weterman MA, Kyllerman M, Smit LM, Kaplan RA, Haas RH, Baas F, Cobben JM, Poll-The BT. Pontine tegmental cap dysplasia: a novel brain malformation with a defect in axonal guidance. *Brain* 2007; **130** (Pt 9): 2258–66
14 Prabowo AS, vanScheppingen J, Iyer AM, Anink JJ, Spliet WG, vanRijen PC, Schouten-van Meeteren AY, Aronica E. Differential expression and clinical significance of three inflammation-related microRNAs in gangliogliomas. *J Neuroinflammation* 2015, **12**: 97–111.
15 Budde BS, Namavar Y, Barth PG, Poll-The BT, Nurnberg G, Becker C, van Ruissen F, Weterman MA, Fluiter K, te Beek ET, Aronica E, van der Knaap MS, Hohne W, Toliat MR, Crow YJ, Steinlin M, Voit T, Roelens F, Brussel W, Brockmann K, Kyllerman M, Boltshauser E, Hammersen G, Willemsen M, Basel-Vanagaite L, Krageloh-Mann I, De Vries LS, Sztriha L, Muntoni F, Ferrie CD, Battini R, Hennekam RC, Grillo E, Beemer FA, Stoets LM, Wollnik B, Nurnberg P, Baas F. tRNA splicing endonuclease mutations cause pontocerebellar hypoplasia. *Nat Genet* 2008, **40**:1113–18.
16 Yee KT, Simon HH, Tessier-Lavigne M, O'Leary DM. Extension of long leading processes and neuronal migration in the mammalian brain directed by the chemoattractant netrin-1. *Neuron* 1999; **24**: 607–22
17 Bloch-Gallego E, Ezan F, Tessier-Lavigne M, Sotelo C. Floor plate and netrin-1 are involved in the migration and survival of inferior olivary neurons. *J Neurosci* 1999; **19**: 4407–20
18 Wingate RJ. The rhombic lip and early cerebellar development. *Curr Opin Neurobiol* 2001; **11**: 82–8
19 Feng X, Juan AH, Wang HA, Ko KD, Zare H, Sartorelli V. Polycomb EZH2 controls the fate of GABAergic neurons in the embryonic cerebellum. *Development* 2016; **143**: 1971–8011
20 Roidl D, Hacker C. Histone methylation during neural development. *Cell Tissue Res* 2014; **356**: 539–52

Supporting information

Additional Supporting Information may be found in the online version of this article at the publisher's web-site:

Figure S1. H3K27me3 immunoreactivity in case 3 (PTCD; pontine tegmental cap dysplasia).
Figure S2. H3K27me3 immunoreactivity in control cerebellum.

Received 12 May 2016
Accepted after revision 7 November 2016
Published online Article Accepted on 25 November 2016